

An *in vivo* study of turbidity suppression by optical phase conjugation (TSOPC) on rabbit ear

Meng Cui,^{1,*} Emily J. McDowell,² and Changhui Yang^{1,2}

¹California Institute of Technology, Pasadena, CA 91125, USA
Department of Electrical Engineering (MC 136-93)

²California Institute of Technology, Pasadena, CA 91125, USA
Department of Bioengineering (MC 136-93),
* mcui@caltech.edu

Abstract: We present a holography-based *in vivo* optical phase conjugation experiment performed on a living rabbit ear. The motion of live tissues caused the phase conjugate signal to decay with a consistent decay time of less than two seconds. We monitor the signal decay time variation after the ear is excised to postulate different mechanisms that cause the signal decay. The experimental findings address the minimum speed limit of a broad range of optical time reversal experiments for *in vivo* applications on tissues.

©2009 Optical Society of America

OCIS codes: (170.3660) Light propagation in tissues; (170.6930) Tissue; (170.6935) Tissue characterization; (170.7050) Turbid media; (090.1000) Aberration compensation.

References and links

1. T. Vo-Dinh, *Biomedical photonics handbook* (CRC press, New York, 2003).
2. V. V. Tuchin, "Optical clearing of tissues and blood using the immersion method," *J. Phys. D Appl. Phys.* **38**(15), 2497–2518 (2005).
3. I. M. Vellekoop, and A. P. Mosk, "Universal optimal transmission of light through disordered materials," *Phys. Rev. Lett.* **101**(12), 120601 (2008).
4. A. Yariv, and P. Yeh, "Phase conjugate optics and real-time holography," *IEEE J. Quantum Electron.* **14**(9), 650–660 (1978).
5. J. Feinberg, and R. W. Hellwarth, "Phase-conjugating mirror with continuous-wave gain," *Opt. Lett.* **5**(12), 519–521 (1980).
6. R. C. Lind, and D. G. Steel, "Demonstration of the longitudinal modes and aberration correction properties of a continuous-wave dye laser with a phase-conjugate mirror," *Opt. Lett.* **6**(11), 554–556 (1981).
7. P. D. Drummond, and A. T. Friberg, "Specular reflection cancellation in an interferometer with a phase-conjugate mirror," *J. Appl. Phys.* **54**(10), 5618–5625 (1983).
8. D. P. M. Gower, *Optical phase conjugation* (Springer-Verlag, New York, 1994).
9. Z. Yaqoob, D. Psaltis, M. S. Feld, and C. Yang, "Optical phase conjugation for turbidity suppression in biological samples," *Nat. Photonics* **2**(2), 110–115 (2008).
10. E. J. McDowell, M. Cui, I. M. Vellekoop, V. Senekerimyan, and Z. Yaqoob, "Turbidity suppression from the ballistic to the diffusive regime in biological tissues using optical phase conjugation," *J. Biomed. Opt.* submitted.
11. K. Jeong, J. J. Turek, and D. D. Nolte, "Volumetric motility-contrast imaging of tissue response to cytoskeletal anti-cancer drugs," *Opt. Express* **15**(21), 14057–14064 (2007).
12. C. Gu, and P. C. Yeh, "Partial phase-conjugation, fidelity, and reciprocity," *Opt. Commun.* **107**(5-6), 353–357 (1994).

1. Introduction

Biological tissues are highly heterogeneous. Optical wave propagation in such media is dominated by elastic scattering [1], which presents significant challenges for tissue optics. Elastic scattering can randomize the optical wavefront, preventing direct imaging through tissues. If there is a way to suppress the random elastic scattering, optical imaging measurements will be straightforward. The physical origin of the random light scattering is that there are many types of structures and substances in tissues and their refractive indices can vary from each other. One promising technique to suppress scattering is to treat the biological tissues with chemicals for reducing the refractive index mismatch, a method known as optical clearing [2]. Alternatively, the input optical field can, in principle, be optimized in terms of its amplitude and phase wavefront to enhance its transmission through the tissue [3].

In fact, results in ref [3] indicate that the transmission through a scattering medium asymptotes to a universal value of $2/3$, regardless of the sample's scattering thickness. This approach is predicated on the fact that elastic scattering of an optical wave may appear random but is actually deterministic in nature. Extending further upon this logic, this determinism property also implies that light scattering is time-reversible. Optical phase conjugation (OPC) is known to be able to time reverse the scattering process and 'heal' wavefront distortions. Although OPC has been an active field since the 1970s [4–8], its application to tissue optics remains largely unexplored. Recently, we demonstrated that holographic recording of the transmission of a single mode laser through chicken tissue, followed by a phase conjugate playback can allow the optical wave to retrace the scattering path [9]. We found that this process, termed turbidity suppression by optical phase conjugation (TSOPC), is surprisingly robust. To date we have been able to perform TSOPC through 7 mm thick excised chicken tissue sections [10]. While such a technique holds great promise in tissue optics, living tissues pose additional challenges.

The challenges associated with living samples can be divided into two main categories: sample motion and sample absorption. Our technique is a two-step process, holographic recording of the scattered wavefront followed by a time reversed playback. The applicability of our technique for *in vivo* work depends on the relative time scales between the optical realization of TSOPC and tissue variation that can perturb the time reversal process. Motion of the scatterers during and after the recording time serves to reduce the portion of the optical wave that is efficiently time reversed. Sample motion arises in living tissues from a variety of sources: microscale active motion due to molecular motors and metabolic processes, bulk motion caused by muscle contractions including the animal's pulse, as well as diffusive or Brownian motion of particles in the fluid environment of the tissue.

An additional challenge arises from the fact that the blood present in living tissues is highly absorptive. Unlike scattering, tissue absorption is an irreversible process. As such, we can categorize absorption as a loss mechanism that eliminates parts of the input light field from phase conjugation considerations. In this context, absorption is similar to tissue backscattering and tissue movements between the process of light field recording and phase conjugation – all are generalized light field information loss mechanism. In a recent study, we have found that as little as 0.02% of the scattered wavefront need be collected for effective reconstruction, provided the sample is highly scattering [10]. This study indicates that the TSOPC process is highly robust and is well capable of handling significant light field information loss. As such, as long as sample absorption is not excessive, TSOPC reconstruction can still occur. Our current study focuses on the impact of sample movement on TSOPC. Absorption in our samples was comparatively low and remained constant in all the experiments.

Tissue motion has been studied on other context for a number of reasons, and has formed the basis of several emerging imaging techniques. Recent publications have shown that tissue motion may be a potential metric of the cellular response to anti-cancer drugs [11]. We are interested in both the effect of tissue motion on our system, and the ability to distinguish viable tissues from non-viable tissues based on our measurements.

2. Experiment

As mentioned above, in the first step of the experiment a collimated laser beam was used to illuminate the ear of a rabbit and record the transmitted light in a hologram. In step two, the phase conjugate of the transmitted light was read out from the hologram and back-propagated through the ear. The transmitted signal was recorded in time and analysis of the signal decay yielded the time scale of the *in vivo* tissue perturbation. We repeated the measurement 0.5, 1, 2, 3, and 24 hours after the ear was excised, which revealed several perturbation mechanisms of different time scales.

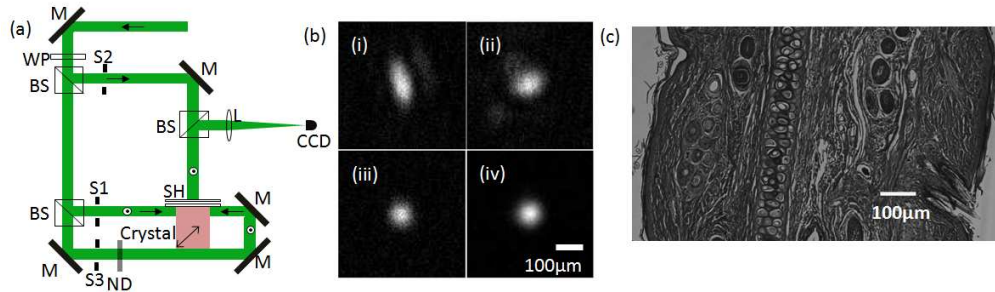


Fig. 1. (a) Top view of the experimental setup of *in vivo* TSOPC. The light source is a solid state CW laser at 532 nm (Spectral Physics, Excelsior). M = mirrors, WP = half wave plate for 532nm, BS = beam splitter, S1,2,3 = shutters, SH = sample holder, L = lens, CCD = CCD camera, ND = neutral density filter, Crystal = 45° cut LiNbO₃ crystal. The dark arrow on top of the crystal shows the c axis of the crystal. The concentric dark ring and dot represent the vertical polarization of the laser beams. The rabbit is held on top of the crystal with a shelf which is not shown. (b) Reconstructed TSOPC images through the ear of the rabbit when it is alive (i, ii) and 30 mins after euthanasia (iii), and through a tissue phantom of comparable scattering property (iv). (c) Histology of the ear of the rabbit.

Figure 1(a) shows the top view of the experimental setup. The collimated output of a solid state CW laser at 532nm (Spectral Physics, Excelsior) was split into three vertically polarized beams: a signal beam, a writing beam, and a reading beam. In the first step, shutter 1 and 2 were open and shutter 3 was closed to pass the signal beam and the writing beam. The signal beam illuminated the sample and the transmitted scattered light interfered with the writing beam inside the 45° cut, iron doped LiNbO₃ photorefractive crystal to form a 3D holographic grating along the c-axis of the crystal. In the next step, shutter 1 and 2 were closed and shutter 3 was opened to pass only the reading beam, which counter-propagated through the crystal with respect to the writing beam and generated the phase conjugate of the recorded scattered wavefront. The transmission of the phase conjugate light through the sample was focused onto a CCD camera. The powers of the signal, writing and reading beams were 48mW, 48mW and 4.8mW, respectively. A 5 second recording time was used throughout the experiments. The reading process in photorefractive materials can erase the stored hologram. Using a power ratio of 1:10 between the reading and writing beams ensured a hologram life time of ~6 min.

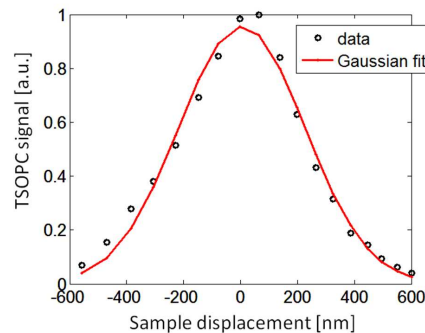


Fig. 2. TSOPC signal vs. sample displacement during playback. The data are fitted with a Gaussian function (red line).

The ear of a New Zealand rabbit under deep anesthesia was gently held between two glass slides and mounted onto the sample holder. Figure 1(b) shows the reconstructed TSOPC images through the ear of the rabbit (histology shown in Fig. 1(c)) when the rabbit was alive (i, ii), 30 mins after euthanasia (iii), and through a tissue phantom of comparable scattering properties (iv). The images reconstructed through the ear of the euthanized rabbit (iii) and the tissue phantom (iv) were similar round spots ~68 micron in diameter as expected from the 1.5

mm input beam diameter and the 150mm lens in front of the camera. The images (i, ii) reconstructed through the live rabbit's ear however deviated from the expected round spot, indicating that the scattering structures in the tissue varied during the recording process (5 sec) and distorted the hologram.

We were interested in measuring the sensitivity of the reconstructed TSOPC signal to tissue variation. To investigate the minimum length scale on which sample perturbations affected the TSOPC measurement, we mounted a 1.6 mm thick tissue phantom composed of polystyrene microspheres (1 micron in diameter, weight concentration 1.77%) suspended in a polyacrylamide hydrogel on a translational stage driven by a piezo actuator. The product of the scattering coefficient of the phantom and the sample thickness was $\mu_s L = 130$. A laboratory-built laser fringe tracking system was employed to monitor the stage position with better than 30 nm accuracy. After the holographic recording (experimental step one), we displaced the sample and monitored the TSOPC signal variation. Figure 2 shows the experimentally measured TSOPC signal decay as a function of sample displacement during TSOPC playback (experimental step two). Gaussian fitting (red line) yields a FWHM of 523 nm which is comparable to the wavelength (532 nm) of the laser used in the experiment. Based on this study, we expect that the vibration caused by heart beat should significantly affect the reconstructed TSOPC signal.

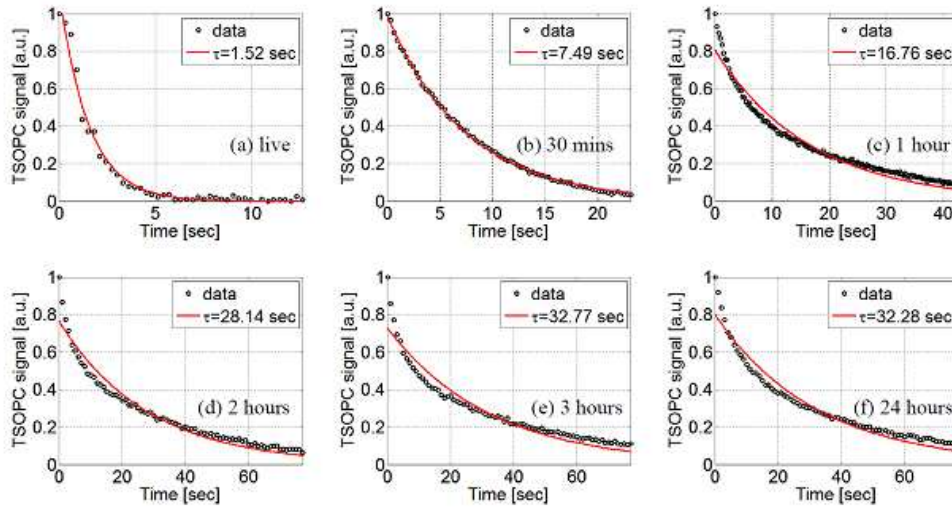


Fig. 3. (a-f) TSOPC signal decay measured when the rabbit is alive and 0.5, 1, 2, 3, 24 hours after the ear is excised. The data are fitted with an exponential function (red line).

Figure 3(a-f) show the TSOPC signal decay curve measured through the living ear, as well as 0.5, 1, 2, 3, and 24 hours after the ear was excised. An exponential function $a \cdot \exp(-t/\tau)$ was used to fit the decay and yield the decay constant τ . As we predicted from Fig. 1(b) (i, ii), the sample perturbation in a living rabbit ear (Fig. 3(a) $\tau = 1.5$ sec) was indeed faster than the holographic recording time (5 sec). After the excision, the decay time quickly increased and then gradually reached a plateau ($\tau = 0.5$ min). To separate the decay caused by the tissue variation from other experimental factors including the hologram decay and the laser and mechanical instabilities, we performed the TSOPC experiment without a scattering medium present, from which we identified a hologram lifetime of 6 min. We then measured the TSOPC signal decay as a function of time for a polyacrylamide tissue phantom with $\mu_s L$ comparable to the ear of the rabbit. The measured decay time ($\tau = 2$ min) is due to the laser and mechanical instabilities of our setup.

After excision of the ear, the decay rate of the TSOPC signal initially drops quickly. We attribute this immediate change to the fact that the heart beat no longer affects the ear of the animal. The heart beat (i.e. pulse) appears to be responsible for tissue vibrations and bulk

motion that move the tissue to a much greater length scale than the optical wavelength. An additional source of motion in the tissue is the microscale motion caused by cells undergoing active processes, varying their shape, size, and location over time. The ear tissue is alive upon excision, but gradually ceases activities as the tissue dies. After ~2 hours, the decay rate reaches a plateau. This plateau, however, is still much faster than the decay rate of the tissue phantom. We attribute this finding to the fluidic environment inside the tissues and associated Brownian motion that exists even when the tissue is not longer living. Unlike the tissue phantoms, the scattering structures of the tissue are not held in place by a hydrogel. Each of these factors can significantly perturb the time reversal process, and each of them has its own time scale.

3. Theory

In the absence of absorption, the time reversal signal can be explained with the reciprocity theorem [12]. We extend the derivation in Ref [12] to spatial frequency domain which is consistent with our experiments since the CCD detector is at the Fourier plane. Let's assume the electric field of the input signal is $E_1(k_x, k_y)$. The transmission through the scattering medium (rabbit ear or tissue phantom) can be written as

$$E_2(k'_x, k'_y) = \int E_1(k_x, k_y) H(k_x, k_y, k'_x, k'_y) dk_x dk_y, \quad (1)$$

where $H(k_x, k_y, k'_x, k'_y)$, a complex number, is the scattering coefficient from input mode (k_x, k_y) to the transmission mode (k'_x, k'_y) . $E_2(k'_x, k'_y)$ is recorded in the photorefractive crystal and a reading beam generates a phase conjugate copy of $E_2(k'_x, k'_y)$ with reversed propagation direction. We can write the phase conjugate field as $E_3(k'_x, k'_y) = R(k'_x, k'_y) E_2^*(k'_x, k'_y)$ where $R(k'_x, k'_y)$, a real number, is the phase conjugate reflectivity. For an ideal phase conjugate device, $R(k'_x, k'_y)$ is a constant number. In practice, $R(k'_x, k'_y)$ is often a function of wave vectors (k'_x, k'_y) . $E_3(k'_x, k'_y)$ propagates back through the scattering medium. Its transmission can be written as

$$E_4(k_x, k_y) = \int E_3(k'_x, k'_y) H'(k'_x, k'_y, k_x, k_y) dk'_x dk'_y. \quad (2)$$

As in Eq. (1), $H'(k'_x, k'_y, k_x, k_y)$ is the scattering coefficient from input mode (k'_x, k'_y) to the transmission mode (k_x, k_y) . According to the reciprocity theorem, for stationary media

$$H'(k'_x, k'_y, k_x, k_y) = H(k_x, k_y, k'_x, k'_y). \quad (3)$$

From Eqs (1), (2) and (3), $E_4(k_x, k_y)$ can be expressed as

$$E_4(k_x, k_y) = \iint R(k'_x, k'_y) E_1^*(k''_x, k''_y) H^*(k''_x, k''_y, k'_x, k'_y) H(k_x, k_y, k'_x, k'_y) dk''_x dk''_y dk'_x dk'_y. \quad (4)$$

In our experiments, the input is a collimated laser beam and we measure the amplitude variation of its phase conjugate, a collimated beam with reversed propagation direction. Suppose the input mode is (k_{x0}, k_{y0}) and its divergence is $(\Delta k_{x0}, \Delta k_{y0})$ and we measure the strength of the phase conjugate signal of this mode, we can approximate the integral in Eq. (4) as

$$E_4(k_{x0}, k_{y0}) = E_1^*(k_{x0}, k_{y0}) \Delta k_{x0} \Delta k_{y0} \int R(k'_x, k'_y) H^*(k_{x0}, k_{y0}, k'_x, k'_y) H(k_{x0}, k_{y0}, k'_x, k'_y) dk'_x dk'_y. \quad (5)$$

Inside the integral of Eq. (5), $R(k'_x, k'_y)$ is a real number and the phases of $H(k_{x0}, k_{y0}, k'_x, k'_y)$ and $H^*(k_{x0}, k_{y0}, k'_x, k'_y)$ strictly cancel, meaning that phase conjugation

causes the transmitted E fields exactly retrace their scattering trajectory and interfere constructively. The derivation of Eq. (5) is based on the assumption that the scattering medium is stationary such that the reciprocity theorem applies (Eq. (3)). For a time varying sample, such as a living rabbit ear, Eq. (3) no longer holds and Eq. (5) becomes

$$E_4(k_{x0}, k_{y0}) = E_1^*(k_{x0}, k_{y0}) \Delta k_{x0} \Delta k_{y0} \int R(k'_x, k'_y) H^*(k_{x0}, k_{y0}, k'_x, k'_y) H'(k'_x, k'_y, k_{x0}, k_{y0}) dk'_x dk'_y. \quad (6)$$

The phases of $H^*(k_{x0}, k_{y0}, k'_x, k'_y)$ and $H'(k'_x, k'_y, k_{x0}, k_{y0})$ could be independent given that the scattering medium has been significantly varied, which cause the integral in Eq. (6) to vanish. By monitoring the amplitude of the phase conjugate signal, we can measure the variation of the function $H(k_x, k_y, k'_x, k'_y)$ over time, which reveals the dynamics inside the scattering medium.

4. Conclusion

In conclusion, we performed *in vivo* TSOPC experiment on a living rabbit ear and monitored the signal decay as a function of time. We repeated the measurement after the ear was excised. The changes in decay time characteristics suggest three possible perturbation mechanisms: bulk motion, microscale cellular motion, and Brownian motion in the fluidic environment. In living tissues, bulk motion due to the heart beat and associated muscle contractions seem to be the dominant perturbation mechanism with the shortest decay time. The experimentally measured 1.5 second decay time showed that TSOPC is promising for *in vivo* applications if a fast time reversal process such as four-wave mixing (FWM) in a Brillouin scattering medium is employed. This finding also provides the minimum experiment time limit for various time reversal based experiments in living tissues.

Acknowledgement

This work was funded by the NIH under Grant No.R21EB008866-02.